Effects of Atmospheric Path on Airborne Multispectral Sensors

ROBERT HORVATH, JOHN G. BRAITHWAITE, and FABIAN C. POLCYN[1] Institute of Science and Technology, The University of Michigan, Ann Arbor, Michigan

Abstract

Experimental data were acquired for a study of the effects of variable atmospheric path on the spectral signals obtained by remote sensors in the optical region of the spectrum. Multichannel optical-mechanical scanners which provide calibrated apparent spectral radiance data were flown over agricultural test sites, and passes were made at several different altitudes between 2000 and 10,000 ft. The quantitative results compare favorably with qualitative theoretical predictions. Optical-mechanical scanners and aerial photographic systems are compared to show the relative importance of potentially detrimental atmospheric path effects with regard to the operation of these systems in remote sensing.

Introduction

Investigators in the field of remote sensing have long been concerned with the effects of altitude on the data acquired. This has been especially true since high-altitude aircraft and satellite platforms became available. Historically, the initial (and so far the greatest) emphasis has been on understanding the manner in which increasing atmospheric path lengths affect the spatial ground resolution attainable with long-focal-length high-resolution camera systems. Even with the advent of optical scanning systems, the emphasis was still on resolution, because classical photointerpretation techniques are based on the common denominator in all such imagery, geometric shape. Concern with the effects of altitude on the apparent intensity of the radiation emanating from the target has usually been restricted to the question of whether or not enough contrast would be present to allow interpretation of geometric "clues." It has become increasingly apparent in recent years, however, that optimum utilization of remote sensing systems requires use of the information contained in the intensity and spectral character of the radiation sensed. In fact, for many applications, knowledge of the spectral distribution of radiation intensity for the object viewed can facilitate identifications or discriminations which would be impossible to make if only the geometric shape were considered. In view of this, it has become increasingly important to understand the effects of variable atmospheric path (resulting from variation in altitude and atmospheric conditions) on spectral intensity distributions. This paper presents the results of an exploratory investigation of the effects of altitude on multispectral data. The investigation was limited to effects relating to the spectral intensity problem, as the effects of altitude on spatial resolution have been well documented elsewhere (e.g., Middleton, 1958).

Theoretical Considerations

Altitude Equation

The effect of sensor altitude on the apparent radiance of a target at the earth's surface which fills the sensor's instantaneous field of view can be ascribed to two simultaneous processes. The matter in the atmospheric path between the target viewed and the sensor (i) attenuates by absorption or scattering the radiation emanating (by reflection or self emission) from the target, and (ii) scatters and emits unwanted radiation into the field of view so that it appears to come from the target. These effects can be shown in equation form as follows: if $L_\lambda{}^t$ is the actual radiance of the target t in a small spectral bandwidth centered at wavelength λ, then the apparent radiance $L^t_{\lambda,h}$ sensed vertically from altitude h is given by

$$L^t_{\lambda,h} = \tau^p_{\lambda,h} L_\lambda{}^t + L^p_{\lambda,h}, \tag{1}$$

where $\tau^p_{\lambda,h}$ is the path transmission coefficient which indicates the degree to which the actual target radiance is attenuated, and $L^p_{\lambda,h}$ is the extraneous radiation emitted or scattered by the atmosphere into the beam and collected by the sensor. The path transmission coefficient and path radiance are functions of λ, h, and the atmospheric conditions. It is of interest to consider the implications of (1) in order to visualize, at least qualitatively, how such an altitude-radiance relationship affects the remote sensor data. In particular, it is of interest to know not only how the apparent radiance of a given target is modified, but also how the radiance difference between two (or more) targets is affected.

In order to observe the effect of altitude on a given target's apparent radiance, the relation in (1) may be differentiated relative to altitude, producing.

$$\frac{\partial}{\partial h}\left(L_h{}^t\right) = \left(L^t\right)\frac{\partial}{\partial h}\left(\tau_h{}^p\right) + \frac{\partial}{\partial h}\left(L_h{}^p\right), \tag{2}$$

where the common subscript λ has been deleted for clarity. Now $\partial\tau_h{}^p/\partial h$ has a negative value since the overall transmission of the path decreases as the path length increases. On the other hand, $\partial L_h{}^p/\partial h$ has a positive value because (except for some unusual circumstances) the amount of radiation scattered or emitted by the atmosphere into the sensor's field of view increases as the amount of matter (atmospheric path) between the sensor and target increases. Consequently, the direction of the net change with altitude of the apparent target radiance will depend on the relative magnitudes of $\partial\tau^p/\partial h$ and $\partial L^p/\partial h$ and ou the magnitude of the actual target radiance. For instance, it can be seen that, if the actual target radiance L^t were quite small, then the positive term $\partial L^p/\partial h$ (2) could well dominate, so that the apparent target radiance $L_h{}^t$ would increase with altitude. Conversely, if the actual target radiance were quite large, then the negative term $\partial\tau^p/\partial h$ could well dominate, thus producing a decrease in apparent radiance with altitude.

The radiance difference between two targets, a and b, of actual radiance L^a and L^b, respectively, is given by

$$\Delta L^{a,b} = L^a - L^b. \tag{3}$$

The effect of altitude on this difference can be seen by using (1) to obtain the apparent spectral radiance difference:

$$\Delta L_h^{a,b} = L_h{}^a - L_h{}^a = (\tau_h{}^p L^a + L_h{}^p) - (\tau_h{}^p L^b + L_h{}^p)$$

or, substituting (3),

$$\Delta L_h^{a,b} = \tau_h{}^p \Delta L^{a,b}, \tag{4}$$

[1]The work reported herein was supported by the National Aeronautics and Space Administration under Grant NsG 715/23-05-071.

where it has been assumed that a and b are close enough together that changes in atmospheric path length or composition can be neglected. Equation (4) indicates that the apparent radiance difference between two targets will be affected only by atmospheric transmission changes as altitude increases and will be independent of the level of path radiance since the latter quantity is a constant addition and cancels in the differencing. As stated previously, the integrated path transmission will decrease with increasing altitude. Consequently, (4) indicates that the apparent radiance difference between two targets will also decrease with increasing altitude.

Atmospheric Models

The expected direction of the variation of apparent target radiance with altitude can be related to the manner of interaction of the radiation and the atmosphere. As stated previously, the atmosphere alters the radiation from the target by either scattering or absorption. The qualitative effects when one of these mechanisms is predominant can be predicted.

Scattering Atmosphere

Suppose that the predominant manner of atmospheric interaction is scattering. The variation of apparent target radiance with altitude will depend on the magnitude of the actual target radiance relative to some average radiance of the surroundings. The surroundings include the atmosphere, clouds, the sun, and any other object from which radiation can reach the matter in the path between the target and the sensor. Three simplified conditions can hold:

1. If the actual target radiance (per unit solid angle) is less than the average radiance of the surroundings (per unit solid angle), then the apparent target radiance must increase with altitude because the radiance from the surroundings available for scattering into the beam is greater than the target radiance available for attenuation. This is the common condition for imagery at wavelengths of less than 3 μm, where most natural targets reflect much less than 100% of the environmental radiation. This situation can also exist for thermal infrared wavelengths if the apparent temperature of the target is less than the average apparent temperature of the surroundings in the particular spectral band.

2. If the actual target radiance is greater than the average radiance of the surroundings, the apparent target radiance will necessarily decrease with increasing altitude since there is not enough extraneous radiation available for scattering into the beam to make up for the actual target radiance scattered out of the beam. Such a situation usually exists only when the target is actively emitting radiation. For thermal wavelengths this situation is common, requiring only that the target have a higher apparent temperature than the average of the surroundings. For wavelengths at which solar radiation dominates (< 3 μm), such a situation usually obtains only when a target actively emits light under low solar illumination conditions (e.g., city lights at night), or possibly when direct solar radiation is specularly reflected by a high-reflectance target.

3. If the actual target radiance is equal to the average radiance of the surroundings, the situation is equivalent to the target being part of an integrating sphere, or "holraum." No variation in apparent radiance with altitude is to be expected since the actual target radiance attenuated by scattering is made up for exactly by the extraneous radiance scattered into the beam.

Absorbing Atmosphere

For an atmosphere which interacts with the target radiation only by absorption, the variation of apparent target radiance with altitude becomes much more straightforward than for the scattering atmosphere. For radiation at wavelengths less than about 3 μm the only effect of the path is to attenuate and thus decrease the apparent target radiance with altitude since, for realistic atmospheric temperatures, the self-emission of the path at wavelengths below 3 μm is negligible. The relationship between the target radiance and the average radiance of the surroundings is of no consequence in this case. For infrared wavelengths greater than 3 μm, however, the atmospheric path can emit significant radiation, and in fact there is an equivalence between the absorptance and emittance of a given path. As a consequence, the relative effect of the path depends only on the relative temperature of the path and of the target. Assuming, for simplicity, a blackbody target and uniform path temperature, if $L^{BB}(T^t)$ is the actual radiance of a blackbody at temperature T^t, then Eq. (1), defining apparent radiance, can be rewritten

$$\begin{aligned} L_h{}^t &= \tau_h{}^p L^t + L_h{}^p \\ &= (1-\alpha_h{}^p)\, L^{BB}(T^t) + \epsilon_h{}^p L^{BB}(T^p) \\ &= L^{BB}(T^t) + \alpha_h{}^p\, [L^{BB}(T^p) - L^{BB}(T^t)] \end{aligned} \tag{5}$$

since, from Kirchhoff's law, $\alpha^p = \epsilon^p$. Thus the apparent target radiance will be greater than, equal to, or less than the actual target radiance, depending on whether the atmospheric path temperature T^p is greater than, equal to, or less than the target temperature T^t. The degree of absorption affects only the magnitude and not the direction of this change.

Real atmosphere

A real atmosphere will affect target radiation by simultaneous scattering and absorption. A comparison of the qualitative aspects of each indicates that, depending on conditions, scattering and absorption can either reinforce or counteract each other in altering the apparent target radiance. It is possible, however, to make some general statements about the relative importance of the two. In the near-ultraviolet and blue portions of the spectrum, for instance, it is observed that scattering is usually predominant. This is due to the high degree of molecular (Rayleigh) scattering, which varies inversely as the fourth power of the wavelength. Conversely, at infrared wavelengths, absorption is often predominant because of the presence of numerous water vapor and carbon dioxide absorption bands. At intermediate wavelengths the relative importance of scattering and absorption can be expected to be dependent on the specific atmospheric conditions.

Experimental Results

The data chosen for analysis were acquired during the summer of 1966 at the Agronomy Farm of Purdue University near Lafayette, Indiana. On 26 July 1966, multichannel imagery was acquired in consecutive passes at altitudes of 6000, 4000, and 2000 ft. On 15 September 1966, multichannel imagery was acquired at five altitudes ranging from 10,000 to 2000 ft. In both cases the altitudes were flown in descending order to minimize the time lapse between the first and last passes. The data analyzed were acquired by a 12-channel scanner which senses in 12 contiguous narrow bands over the wavelength range from 0.4 to 1.0 μm. Table I shows the spectral range for each of the 12 channels. These data were calibrated at the time of acquisition, so that subsequent processing in the laboratory produced apparent spectral radiance distributions for the targets of

Table I
Spectral bandwidths of the 12-channel spectrometer[a]

Spectrometer channel	Spectral bandwidth (μm)
1	0.404–0.437
2	0.437–0.464
3	0.464–0.482
4	0.482–0.502
5	0.502–0.524
6	0.524–0.549
7	0.549–0.580
8	0.580–0.617
9	0.617–0.659
10	0.659–0.719
11	0.719–0.799
12	0.799–1.000

[a]Defined for 50% response level.

interest. The complete multichannel scanning system and the processing procedure used are described in the Appendix. Absolute apparent radiances as a function of spectrometer channel and altitude were obtained for maturing soybeans and winter wheat stubble on 26 July and for mature corn and wilting soybeans on 15 September. The type of data obtained can be

Insert Fig. 1a Fig. 1b Fig. 2a and 2b hereabouts

seen in Figs. 1 and 2. It should be noted that these curves are not continuous spectral representations, as each channel measures the average radiance in a relatively wide band, and the straight lines connecting individual channels have been drawn only for convenience. There are, however, recognizable spectral shapes. For example, for the maturing soybeans (Fig. 1a), expected radiance peaks appear in the green (channel 8) and near infrared (channels 11 and 12), separated by channels of reduced response which include the chlorophyll absorption region.

Variation in Apparent Radiance

Variations in apparent spectral radiance with altitude can be seen in Figs. 1 and 2, but general trends are better indicated by Figs. 3 and 4, which present the data in terms of normalized radiance (radiance ratio) versus altitude. The normalization for each spectral channel is relative to the apparent spectral radiance at 2000 ft for that channel:

$$\text{Normalized radiance} = \frac{L_h}{L_{2000}}. \quad (6)$$

Such a ratio provides a more straightforward means of comparing the relative change with altitude in apparent radiance among the several spectral bands.

Figure 3 shows curves from the 26 July run. In general, the ratio (and thus the apparent radiance) is seen to increase with altitude in all spectral channels, the increase being more prominent at the shorter wavelengths (lower-numbered spectrometer channels). Comparison with the theory previously presented indicates that, for these data, scattering and not absorption was the dominant atmospheric effect; the inverse variation of the magnitude of this phenomenon with wavelength iscommensurate with scattering theory.

Figure 4 shows curves from the 15 September run. Although

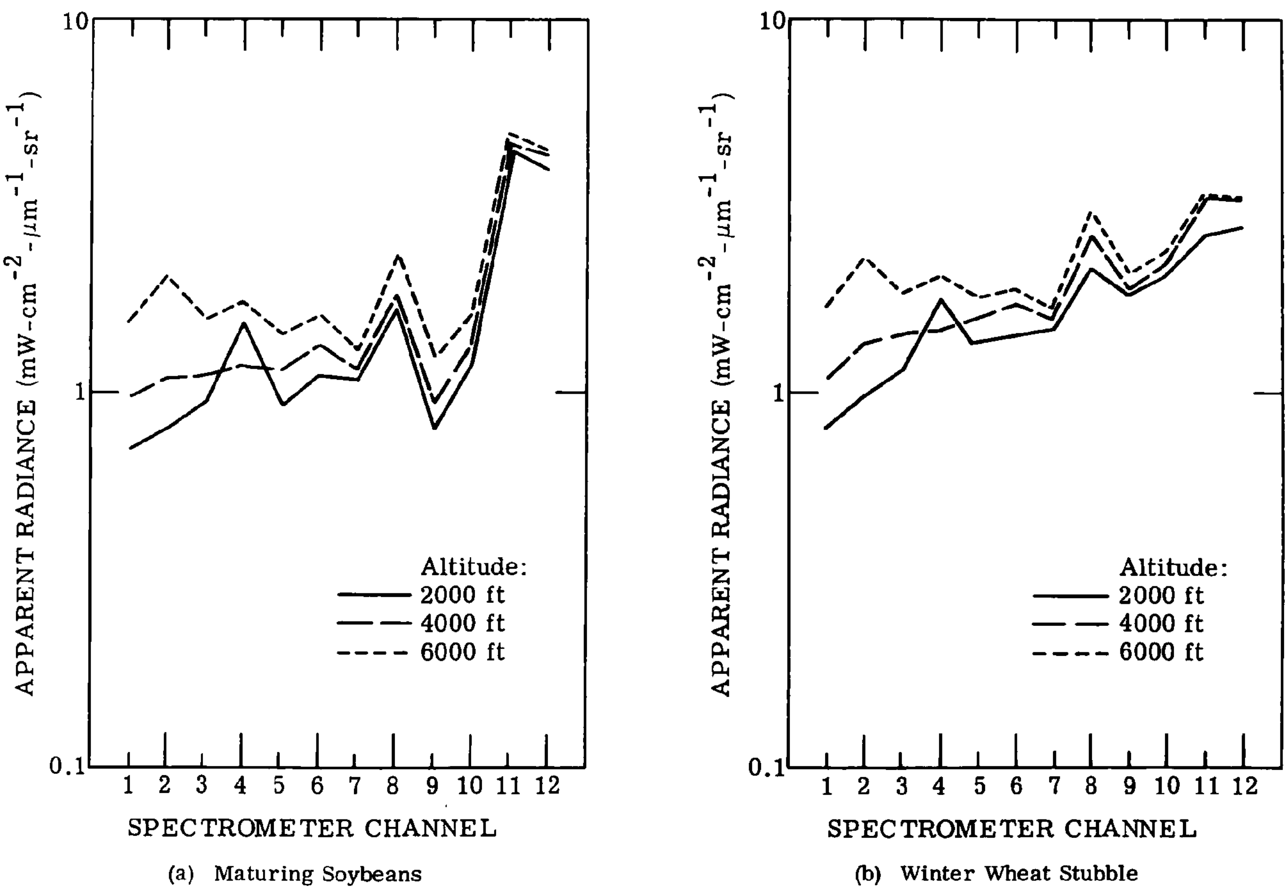

Fig. 1. Apparent spectral radiance of maturing soybeans and wheat stubble. Data acquired 26 July 1966 under hazy but cloudless sky conditions.

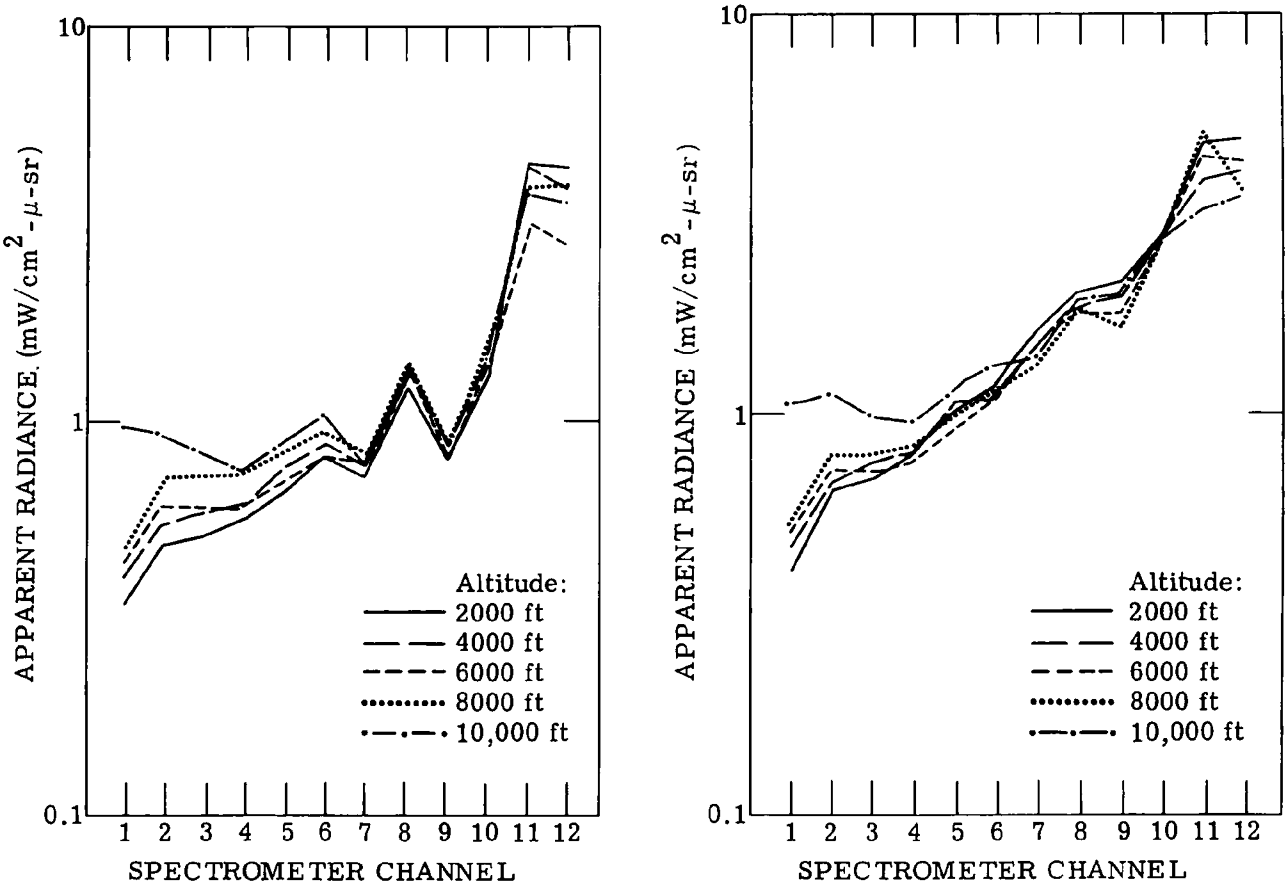

(a) Mature Corn

(b) Wilting Soybeans

Fig. 2. Apparent spectral radiance of mature corn and wilting soy-beans. Data acquired on 15 September 1966 under clear, cloudless sky conditions.

the spectral ordering is similar to that in Fig. 3, there is a tendency for the radiance ratio to *decrease* with altitude at the longer wavelengths. It is not known if this phenomenon is real, however. The intensity of solar illumination increased considerably between the flights at 10,000 ft (0850 hours) and 2000 ft (0947 hours). An attempt was made to compensate for this illumination change at each altitude by using ground-based solar illumination measurements to correct the measured radiances to a common illumination condition. The correction procedure was necessarily approximate since the ground measurements were made by a very broadband instrument, and the spectrally integrated values had to be divided theoretically into contributions from each of the 12 spectral bands represented in the spectrometer. The trends in Fig. 4 *could* be real, however, indicating that, for the longer wavelengths, the attenuation of the actual target radiance might well overcome the tendency of extraneous radiation to increase the apparent radiance with altitude. Such a condition could mean that scattering had less effect on these data than on those taken on 26 July.

The apparent differences between the results in Figs. 3 and 4 can probably be ascribed to the atmospheric conditions. On 26 July the atmosphere was quite hazy, whereas on 15 September it was clear with no discernible haze. Consequently, the effects of scattering should indeed have been greater on 26 July than on 15 September, thus leading to an increased amount of extraneous radiation in the apparent radiances and an increase in those radiances with altitude. The fact that attenuation also increases as scattering increases does not necessarily alter this conclusion.

In describing the altitude equation, it was stated that the direction of change with altitude of apparent radiance depends on the magnitude of the actual target radiance in such a way that, the larger the actual target radiance, the less positive is

Table II
Difference in actual target radiance compared with difference in apparent radiance ratio for Wheat Stubble and Soybeans[a]

Spectrometer channel	$L^{wheat} - L^{soybeans}$	$\frac{L^{wheat}_{6000}}{L^{wheat}_{2000}} - \frac{L^{soybeans}_{6000}}{L^{soybeans}_{2000}}$
1	+	−
2	+	−
3	+	−
4	+	−
5	+	−
6	+	−
7	+	−
8	+	−
9	+	−
10	+	−
11	−	+
12	−	+

[a]Data acquired 27 July 1966.

the change. This was implied in (2) since $\partial\tau_h{}^p/\partial h$ is negative. Similarly, if the radiance ratio were differentiated with respect to altitude, the same relationship would hold, because the denominator of the ratio is a constant with respect to altitude. Thus, if for two targets, a and b,

$$L^a > L^b, \tag{7}$$

it must follow that, for $h > 2000$ ft,

$$\frac{L_h^a}{L_{2000}^a} < \frac{L_h^b}{L_{2000}^b}, \tag{8}$$

since the apparent radiance of target a must change less positively with increasing altitude than the apparent radiance of target b. Tables II and III summarize the results of such a comparison for the 26 July and 15 September data, respectively. In each table the second column indicates whether the difference between the actual radiances of the crops is positive or negative, and the third column indicates whether the difference between the respective radiance ratios as presented in Figs. 3 and 4 is positive or negative. The general results shown in these tables are in obvious agreement with the relations in inequalities (7) and (8); i.e., the sign of the difference in actual target radiance is opposite to the sign of the difference in radiance ratio. The one exception to this is in the data for spectrometer channel 4 in Table II, where the radiance ratios for soybeans and wheat stubble are identical even though the actual radiances are not. No explanation has been found for this anomaly, but it is evident from Figs. 1 and 3 that spectrometer channel 4 behaves quite suspiciously for the data acquired at 2000 ft on 26 July. It

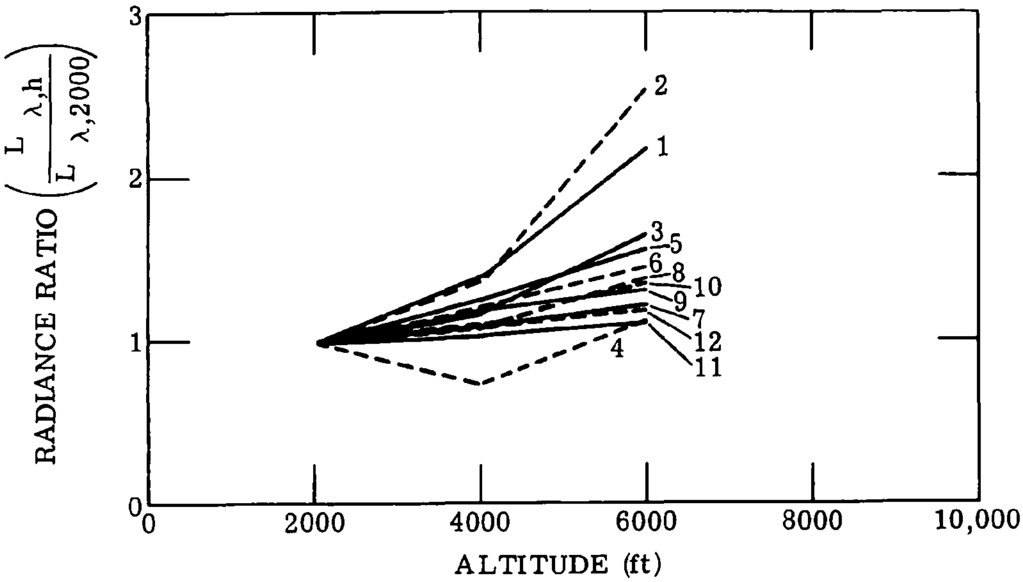

(a) Maturing Soybeans

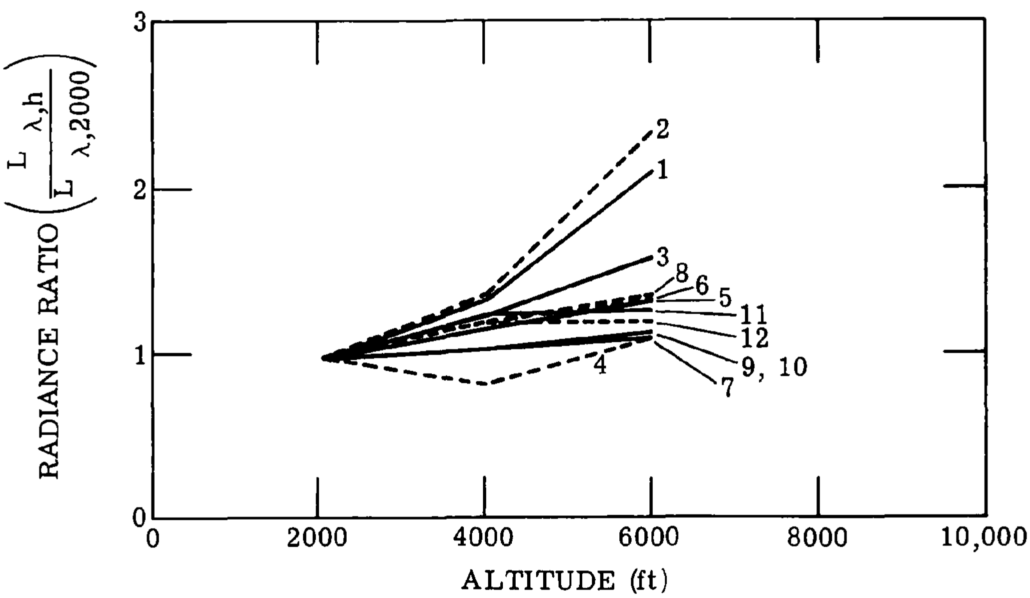

(b) Winter Wheat Stubble

Fig. 3. Radiance ratio versus altitude for maturing soybeans and wheat stubble. Parameter is spectrometer channel.

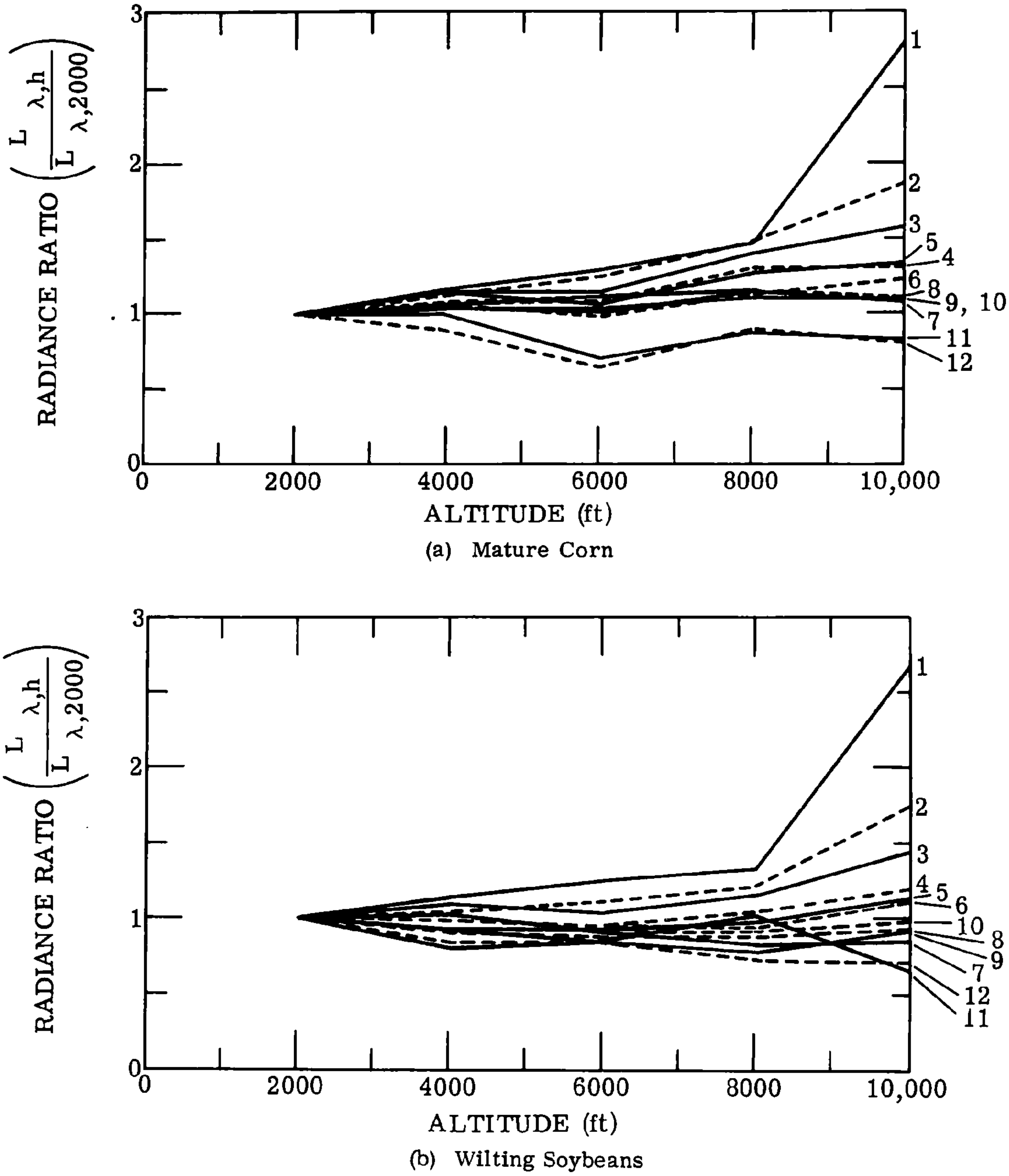

Fig. 4. Radiance ratio versus altitude for mature corn and wilting soybeans. Parameter is spectrometer channel.

Table III
Difference in actual target radiance compared with Difference in apparent Radiance Ratio for Corn and Soybeans[a]

Spectrometer channel	$L^{corn} - L^{soybeans}$	$\frac{L^{corn}_{10,000}}{L^{corn}_{2000}} - \frac{L^{soybeans}_{10,000}}{L^{soybeans}_{2000}}$
1	−	+
2	−	+
3	−	+
4	−	+
5	−	+
6	−	+
7	−	+
8	−	+
9	−	+
10	−	+

[a]Data acquired 15 September 1966.

should be noted that Table III does not contain entries for spectrometer channels 11 and 12. The excessive noise present in the reduction of the data for these channels precluded unambiguous determination of the sign of the difference in actual radiance between the corn and soybeans.

Variation in Apparent Radiance Difference

In the foregoing discussions the combined effect of attenuation loss and extraneous radiation gain on the apparent radiance of a target and the relative effect of the magnitude of the actual target radiance on the direction of change with altitude have been shown. The effect of attenuation alone may be studied by observing the apparent radiance difference between two targets as a function of altitude. As indicated by Eq. (4), the apparent radiance difference between two targets varies directly with the path transmission function and is independent of the extraneous path radiance. Thus, theoretically, the apparent radiance difference must decrease (or at best remain constant) with altitude, since the atmospheric transmission function must decrease (or remain constant) as the path length increases. Figures 5 and 6 show the apparent spectral radiance differences, as a function of altitude, for the crops scanned on 26 July and 15 September, respectively.

For Fig. 5, passes were made at 2000, 4000, and 6000 ft. It is difficult to define any trend in these curves. For some spectrometer channels the radiance difference decreases slightly with altitude, for some it appears to increase slightly, and for still others it varies ambiguously. These results indicate that, for the hazy conditions that obtained on 26 July, any change in τ_h^p between 2000 and 6000 ft was insignificant when compared to the uncertainties in the data caused by system noise, sampling techniques, calibration uncertainties, or the possible slight differences in illumination at the three altitudes.

In Fig. 6 (ignoring for the moment the data acquired at 10,000 ft), the variation with altitude appears to be systematic. In general, the apparent radiance difference decreases with altitude to such an extent that at 8000 ft the apparent difference (and thus τ_h^p) is only one-half the value at 2000 ft. Such a significant variation with altitude for the clear conditions on 15 September seems rather odd when no such variation was noted for the hazy conditions on 26 July (Fig. 5), under which variation would be more likely to occur. As discussed earlier, this apparent effect might be due to some systematic error involved in accounting for the significant illumination changes known to have taken place during the flights of 15 September. The nonsystematic behavior of the data from the pass at 10,000 ft may also be due to such error. In any case, it is felt that the data in Fig. 5 were less subject to uncertainties and systematic errors and thus are probably more indicative of the real variation of τ_h^p with altitude for the conditions covered than the data in Fig. 6; i.e., τ_h^p variations are small compared to the noise and uncertainties introduced by the scanner, calibration, and data processing systems.

Discussion

We have seen how the apparent spectral radiance of a target can vary as a function of altitude. We now consider the effects of such variation on the operation of both scanner and camera airborne remote sensor systems.

Scanner Operational Effects

Signal variation

Optical-mechanical scanners use detectors which transform the radiation signal into a voltage. A simplified representation of this process would be as follows (again implicitly assuming the spectral dependence of all quantities):

$$V_h^t = RL_h^t + V^0, \tag{9}$$

where V_h^t=recorded voltage from system at altitude h looking at target t, R=responsivity of system, L_h^t=apparent radiance of target, and V^0=arbitrary dc voltage applied. Using Eq. (1), Eq. (9) may be expanded to

$$V_h^t = R\tau_h^p L^t + RL_h^p + V^0. \tag{10}$$

From (10), it follows that, since R and V^0 can be arbitrarily selected by changing the electronic gain and dc offset of the system, respectively, it is possible to negate any change in the path transmission coefficient τ_h^p by changing R, and to eliminate completely the effect of the extraneous path radiance by choosing $V^0 = RL_h^p$. As a consequence, then, it would seem that an optical-mechanical scanner system could compensate for any effects of altitude on signal strength, thus maintaining the signal output within the optimum dynamic range for recording. Such flexibility to optimize signal recording does not in any way eliminate the need to account for these atmospheric effects when the data are subsequently processed and interpreted.

Signal-to-Noise Variation. In practice, optimum utilization of the preceding characteristics of a scanner system is ultimately limited by noise considerations. The signal-to-noise ratio (SNR) of the recorded information can be reduced as the effects of the atmospheric path on the target radiance increase. For the purpose of this discussion let the information in which we are

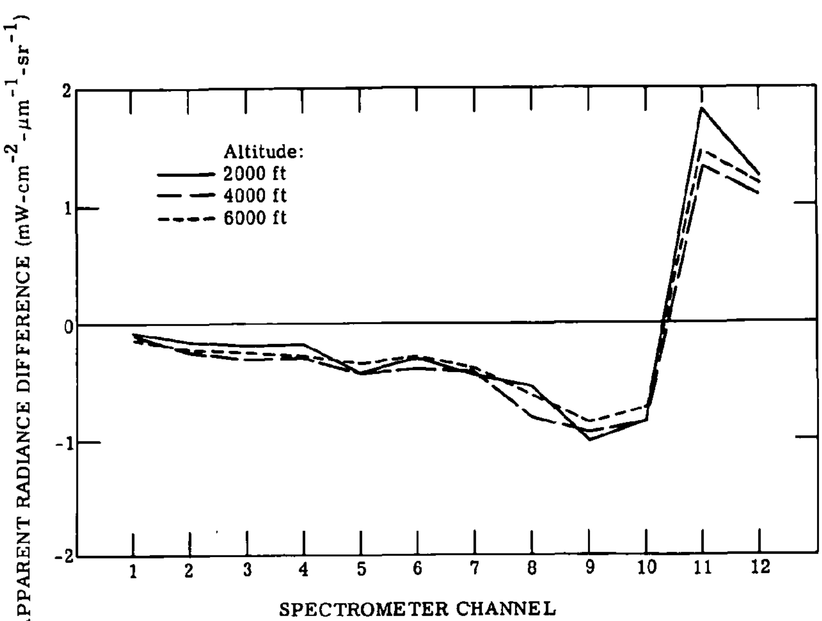

Fig. 5. Apparent spectral radiance difference between maturing soybeans and wheat stubble.

interested be the recorded voltage difference between the two targets, a and b, between which we wish to discriminate. The SNR can then be defined as

$$\mathrm{SNR} = \frac{V_h^a - V_h^b}{\Delta V^n} = \frac{R\tau_h{}^p\, \Delta L^{a,b}}{\Delta V^n}, \tag{11}$$

where V_h^a and V_h^b are as defined above, ΔV^n is the noise voltage, and $\Delta L^{a,b}$ is the actual radiance difference between a and b as defined by Eq. (3). The operational implications of (11) depend on the limiting-noise source producing ΔV^n. Three general conditions can obtain: background noise limiting, detector noise limiting, and system noise limiting.

Background Noise Limiting. A background-noise-limited system is theoretically the optimum system. The limiting noise is produced by the intrinsic statistical fluctuation in arrival rate of photons at the detector from the background. The background is composed of the atmosphere, spectral filter, window material, mirrors, and other objects besides the target in the instantaneous field of view. According to Bose-Einstein statistics, the mean square fluctuation in the number of photons is proportional to the average number of photons. Thus the rms noise equivalent radiance variation is proportional to the square root of the average radiance (Holter *et al.*, 1962), and the SNR relation of (11) becomes

$$\mathrm{SNR} = \frac{R\tau_h{}^p \Delta L^{a,b}}{Rk(\bar{L}_h)^{1/2}} = \frac{\tau_h{}^p\, \Delta L^{a,b}}{k(\bar{L}_h)^{1/2}}, \tag{12}$$

where $\bar{L}_h$ is the average radiance on the detector, and k is a constant. Thus not only will any decrease in $\tau_h{}^p$ with altitude decrease the SNR, but also any increase in apparent target radiance will further decrease the SNR. Equation (12) should not be construed to imply that a decrease with altitude in apparent target radiance will increase the SNR, since any decrease in $\bar{L}_h$ must be caused by a decrease in $\tau_h{}^p$. The best possible condition would be when $\bar{L}_h$ decreases proportionally with $\tau_h{}^p$, at which time the SNR would still decrease at a rate proportional to $(\tau_h{}^p)^{1/2}$.

Detector Noise Limiting. A detector can introduce noise into the signal in several ways, depending on the type of detector and its operating conditions. In general, the magnitude of the noise is stated in terms of an equivalent fluctuation in energy incident on the detector. Consequently, the SNR relation of (11) for a detector-noise-limited system becomes

$$\mathrm{SNR} = \frac{R\tau_h{}^p\, \Delta L_h^{a,b}}{R\Delta L^n} = \frac{\tau_h{}^p\, \Delta L_h^{a,b}}{\Delta L^n}, \tag{13}$$

where ΔL^n is the constant noise equivalent radiance fluctuation at the detector. Thus the variation of the SNR with altitude depends only on the atmospheric attenuation (not on the magnitude of the average radiance, as with the background-noise-limited condition). However, even though this indicates that, for some conditions, the SNR for a detector-noise-limited system can vary less with altitude than a background-noise-limited system, it must be noted that the SNR for the former is inherently lower and remains lower.

System Noise Limiting. In general terms, system noise is any noise entering the signal from the detector output through the recording medium. It takes the form of a noise voltage of some magnitude at the output of the component which produces it. The lumped effect of such noise can be described in a form identical with (13) but with ΔL^n a noise-equivalent radiance which depends on and can vary with the specific operating point of each component in the system. System-noise-limited operation produces inherently lower SNR than either of the situations above.

Photographic Operational Effects

Signal Variation

Cameras use radiation-sensitive films as detectors which transform the apparent spectral radiance of a target into a distribution of opaque silver grains on a base material. The normal measure of intensity for such a system is the optical density of the exposed film. For that portion of the film's dynamic range in which the density is a linear function of the logarithm of the exposure

$$D_h{}^t = \gamma \log R' L_h{}^t + \log E^0 = \gamma \log \frac{R' L_h{}^t}{E'}, \tag{14}$$

where $D_h{}^t$ = recorded optical density from the system at alti-

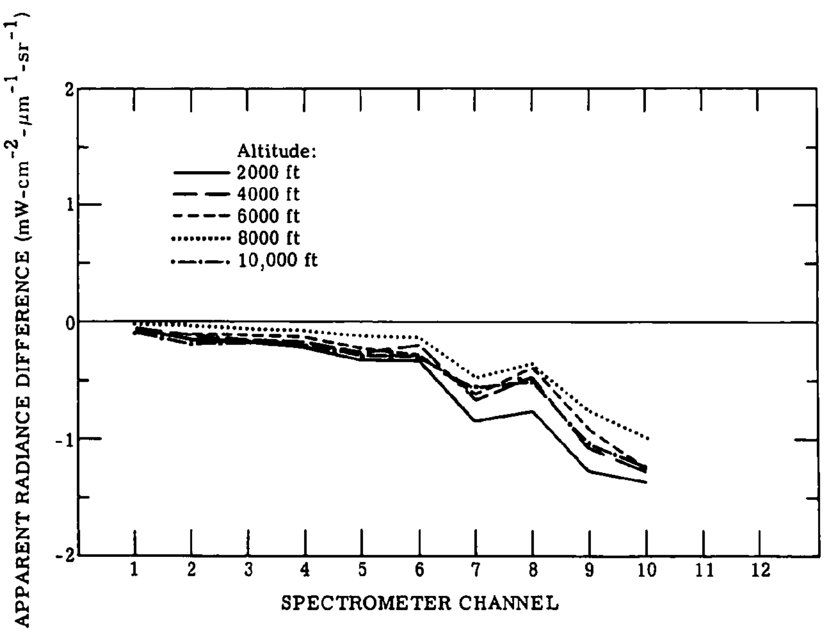

Fig. 6. Apparent spectral radiance difference between mature corn and wilting soybeans.

tude h looking at target t, R' = responsivity of the system, relating radiance to exposure (includes f number and shutter speed), L_h^t = apparent radiance of target, $E^0 = (E')^\gamma$ = intercept of the linear portion of the film curve with the exposure axis (dependent on film type and development conditions), and γ = slope of linear D versus log E curve (dependent on film type and development conditions). Using the relation in Eq. (1), Eq. (14) may be expanded to

$$D_h^t = \gamma \log \frac{R'(\tau_h^p L^t + L_h^p)}{E'}. \qquad (15)$$

Because of the logarithmic response of the photographic emulsion, (15) is quite different from (10), which describes the signal from an optical-mechanical scanner. Although variations in apparent radiance with altitude for a specific target can be compensated for by changes in R' or γ, for example, this is not nearly so easy as the analogous operation with an electrical scanner signal because of the difficulty in monitoring D_h^t directly. In addition, for a camera there is no easily controllable dc offset which can be used to compensate directly for L_h^p, as can be done with the dc voltage offset for a scanner. Consequently, the operational constraints imposed on a camera are somewhat more restrictive than those imposed on a scanner with signals in electrical form.

Signal-to-noise variation

As indicated earlier, the ability to compensate for the effects of variable atmospheric path on apparent target radiance is limited by noise considerations. For a photographic system, the SNR for discriminating between two targets, a and b, can be defined as

$$\text{SNR} = \frac{D_h^a - D_h^b}{\Delta D^n}, \qquad (16)$$

where D_h^a and D_h^b are the recorded densities of targets a and b as defined by (15), and ΔD^n is the noise density variation. From a theoretical viewpoint, it is possible to define the same noise conditions for a camera system as for an optical-mechanical scanner system. As a practical matter, however, especially in view of the envelope of operating conditions for aerial cameras, the only noise condition with which we need be concerned is detector (film) noise limiting.

The noise associated with a photographic emulsion (often called "grain noise," or "granularity") is due to the fact that the apparently homogeneous emulsion is really composed of discrete silver grains with generally random distribution. It can be shown (Higgins and Stulte, 1959) that the rms noise level in a density measurement is proportional to the square root of the density:

$$\Delta D^n = k' D^{1/2}, \qquad (17)$$

where the proportionality constant k' depends on film type, development procedure, and the area over which a particular measurement of density integrates. Using the definition of density in Eq. (14), Eq. (17) becomes

$$\Delta D^n = k' \left(\gamma \log \frac{R'\bar{L}_h}{E'}\right)^{1/2}, \qquad (18)$$

where $\bar{L}_h$ is the average radiance used to expose a particular portion of the film. Substituting (18) in the SNR relation of (16)

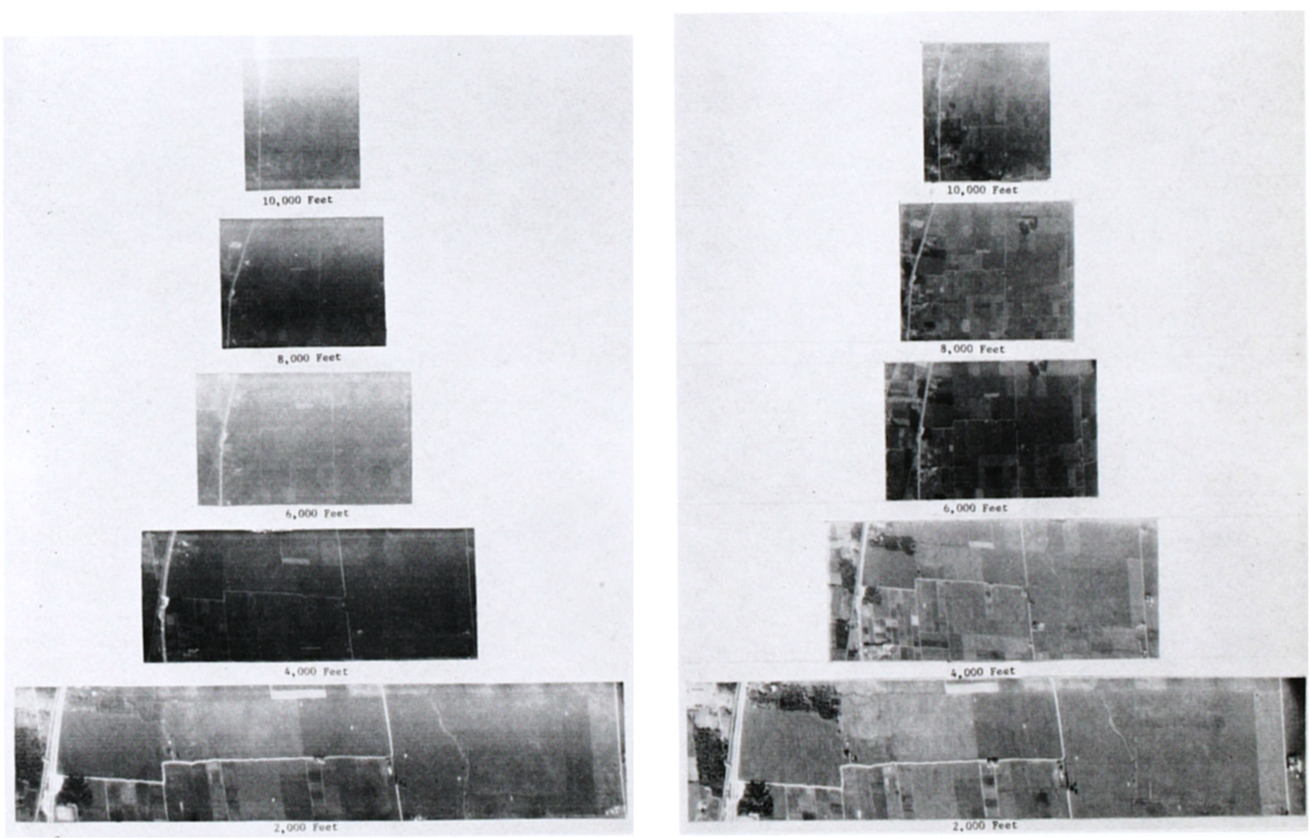

Fig. 7. Comparisons of scanner imagery for various wavelengths at several altitudes. Data acquired 15 September 1966 between 0850 and 0947 hours near the Purdue University Agronomy Farm. (a) 0.32–0.38 μm. (b) 0.404–0.437 μm, channel 1.

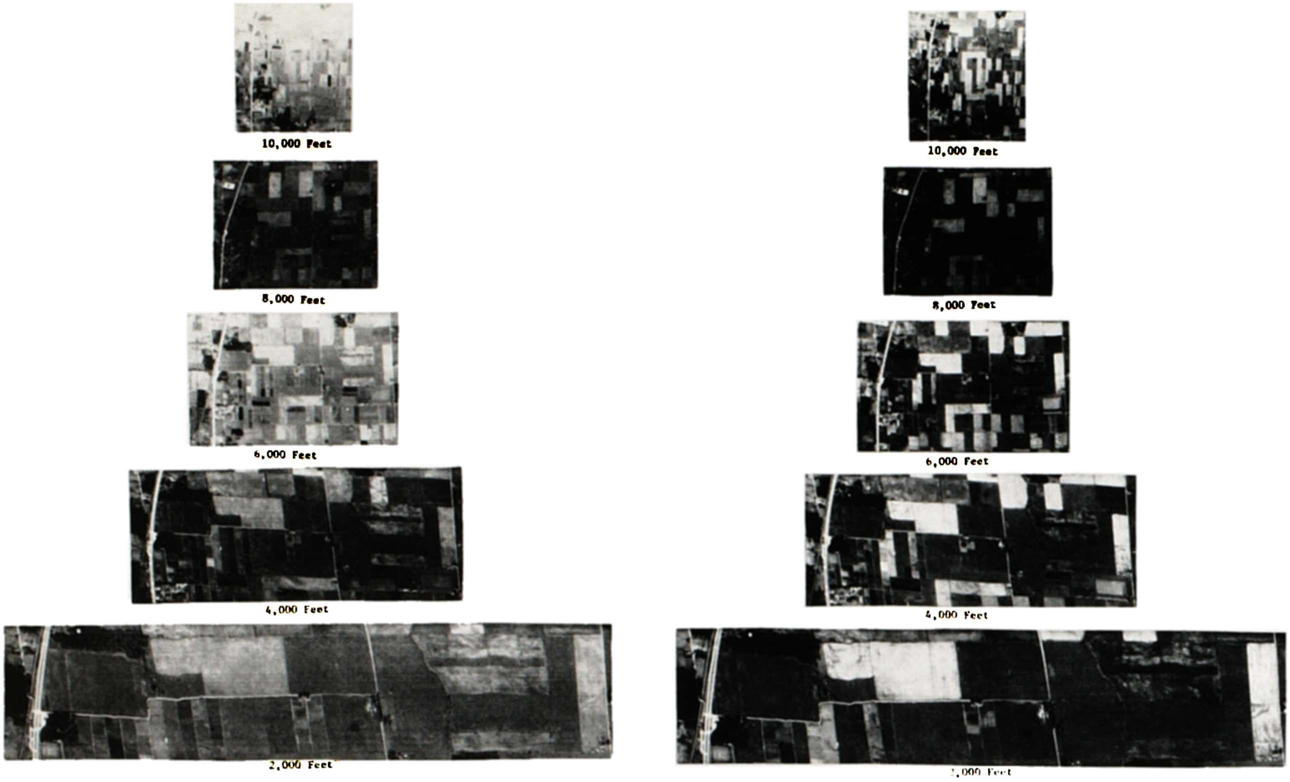

Fig. 7. (*Continued*). (c) 0.549–0.580 μm, channel 7. (d) 0.617–0.659 μm, channel 9.

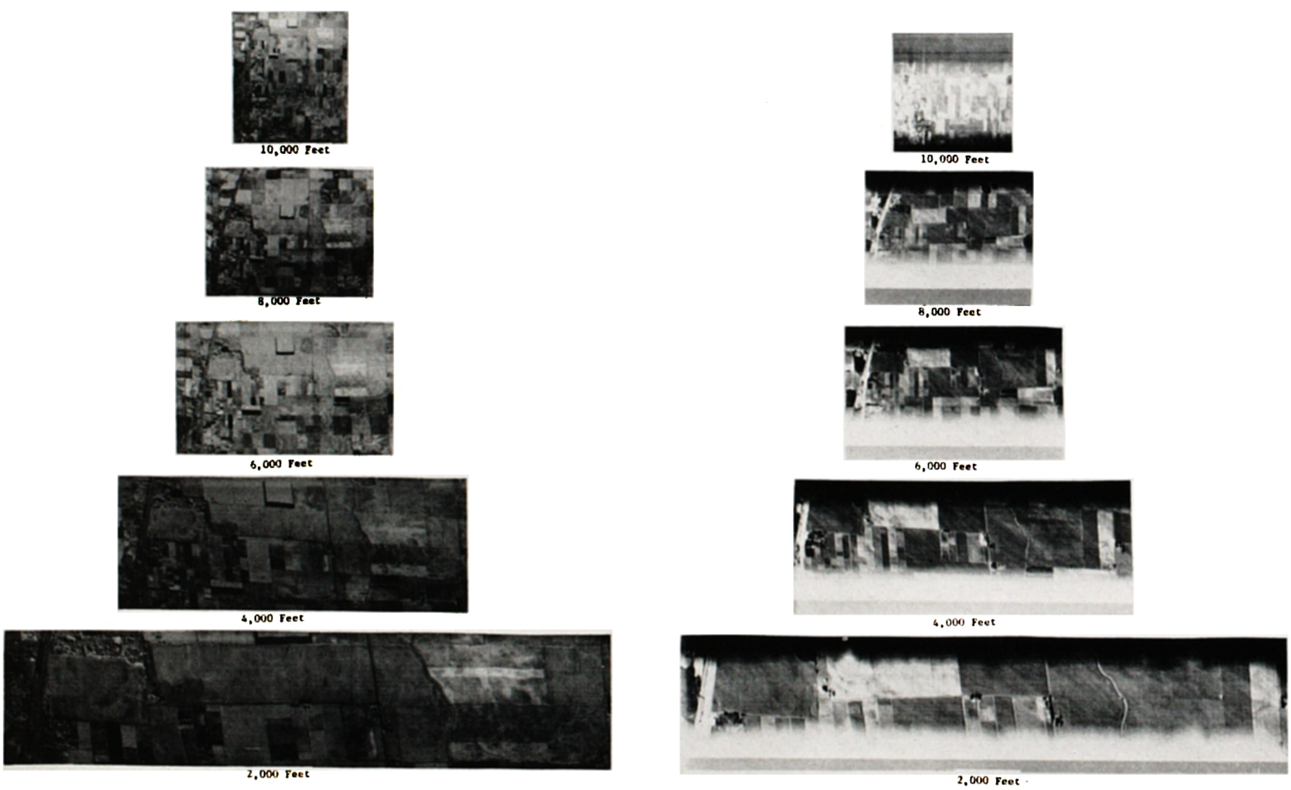

Fig. 7. (*Continued*). (e) 0.799–1.0 μm, channel 12. (f) 8.0–13.5 μm.

and expanding and combining the density terms in the numerator leads to

$$\mathrm{SNR} = \frac{\gamma \log\left(\frac{\tau_h{}^p L^a + L_h{}^p}{\tau_h{}^p L^b + L_h{}^p}\right)}{k'\left(\gamma \log \frac{R'\bar{L}_h}{E'}\right)^{1/2}}. \tag{19}$$

Equation (19) may be simplified somewhat by assuming that the apparent radiance difference between targets a and b is small compared to their average value (the case in which noise considerations are most significant). A binomial expansion of the terms in the logarithm of the numerator of (19) then leads to

$$\mathrm{SNR} = \frac{\gamma \log\left(1 + \frac{\tau_h{}^p \,\Delta L_h^{a,b}}{2\bar{L}_h}\right)^2}{k'\left(\gamma \log \frac{R'\bar{L}_h}{E'}\right)^{1/2}}. \tag{20}$$

Comparison of (20) and (13) indicates that there is a distinct qualitative difference in detector noise limitation between photographic and electronic systems. In an electronic system the SNR decreases *only* as atmospheric transmission decreases; in a photographic system the SNR also decreases because of atmospheric radiance effects, which tend to increase $\bar{L}_h$. As indicated previously, R' can be varied to accommodate changes in $\bar{L}_h$ and maintain the signals in the same density range on the film. This would indeed keep the denominator of (20) constant but would not compensate for any decrease of the numerator due to an increase in $\bar{L}_h$. If R' is reduced even further, it appears that it can in fact compensate completely for atmospheric effects on the SNR. However, large reductions in R' will tend to decrease the dynamic range of the recorded data, since lower-level signals will be forced onto the nonlinear portion of the film response curve and become lost in the fog level of the film. In any event, even though the SNR for a photographic system may degrade relatively faster with increasing altitude than the SNR for a scanner system, it must be remembered that which of these systems gives the higher absolute SNR depends on the particular characteristics of each and on the conditions of data acquisition.

Imagery Examples

It has been stated that changes in apparent target radiance with varying atmospheric path can be compensated for quite easily in an optical-mechanical scanner because of the electrical form of the signals. This is illustrated by the imagery in Fig. 7a to 7f, taken at five different altitudes for four of the spectrometer channels and for the 0.32– to 0.38– μm ultraviolet and 8.0– to 13.5– μm thermal infrared regions. Note that the general quality of the imagery in regard to contrast does not vary significantly with altitude, nor is there any apparent level shift due to increasing path radiance. Even in the ultraviolet (Fig. 7a), where atmospheric scattering effects are extreme, little contrast is lost on account of increasing altitude except for some of the roads whose responses are diminished because of spatial resolution limitations. Generally the upper portions of the shorter-wavelength images appear brighter than the lower portions. This is not an atmospheric effect; rather it is due to the fairly low sun elevation which produced backscattered light

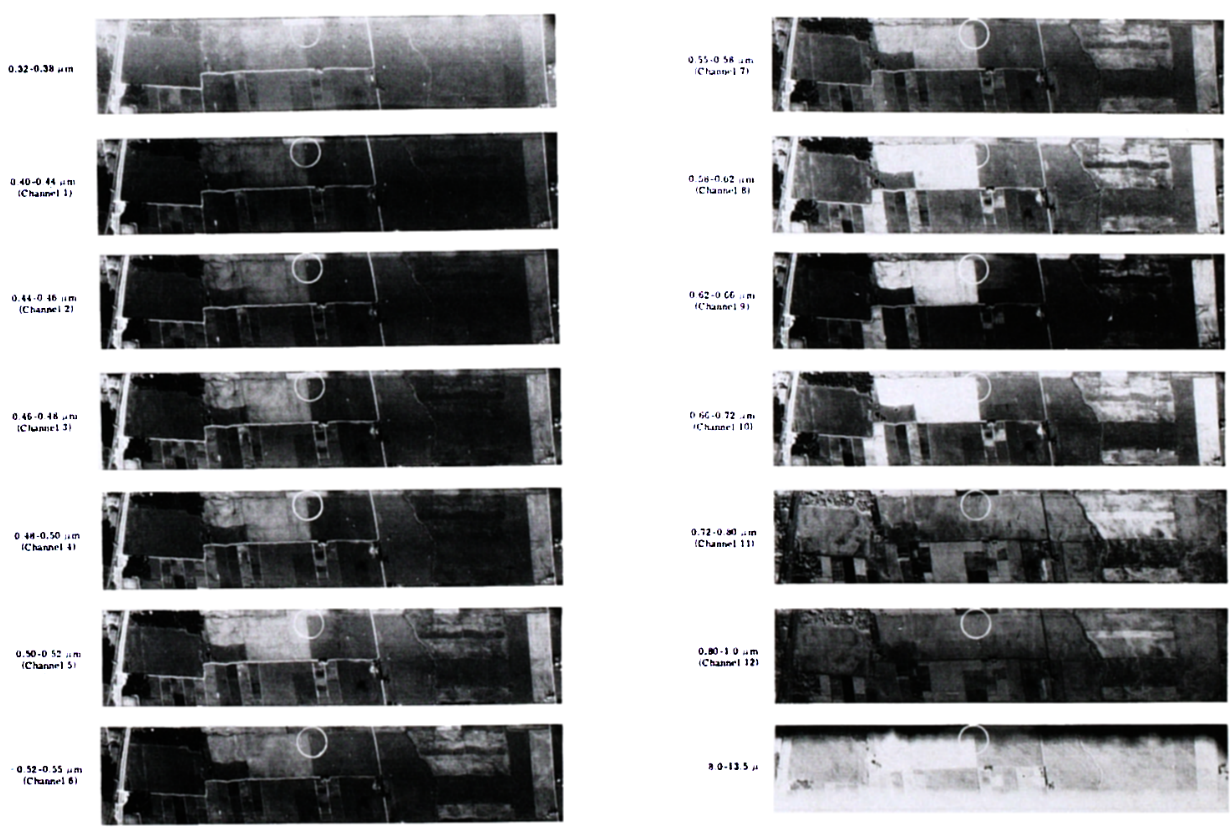

Fig. 8. Scanner imagery taken at an altitude of 2000 ft. Data acquired at 0947 hours on 15 September 1966.

from the terrain in the upper portions and forwardscattered light from the terrain in the lower portions. For agricultural targets, backscattering reflectance is normally higher than forwardscattering reflectance (Malila, 1968). In the 8.0– to 13.5– μm imagery of Fig. 7f, the apparent tonal gradations at the top and bottom of each image are due to vignetting of the field of view caused by the calibration plates (see the Appendix).

The experimental results presented previously indicate that atmospheric effects should not significantly alter spectral differences between targets. Figure 8 shows multispectral imagery of the same agricultural area taken at an altitude of 2000 ft, and Fig. 9 shows imagery of this area taken at 8000 ft. Comparison of Figs. 8 and 9 shows that spectral characteristics are not altered by a change in altitude; except for scale, the features of the imagery are identical. Note, for example, the relative spectral variations of the three fields which meet in the circled area in both figures. The subtle spectral differences at intermediate wavelengths are maintained just as truly at both altitudes as are the gross differences at the shorter and longer wavelengths.

Conclusions

The results of this study in the 0.4– to 1.0– μm spectral region indicate that variations in sensor altitude and acquisition conditions can significantly alter the apparent spectral radiance of a given target. The following conclusions are indicated:

1. An increase in sensor altitude can either increase or decrease apparent target radiance.

2. The tendency toward increase in apparent radiance is inversely related to wavelength.

3. The tendency toward increase in apparent radiance is significantly strengthened by hazy atmospheric conditions.

4. The greater the actual target radiance, the less is the tendency toward increase in apparent radiance with altitude.

5. The attenuation of spectral radiance differences between objects with variation in altitude may not be significant when compared to the noise and uncertainties of present operational systems below 10,000 ft.

6. The decrease with altitude in recorded signal difference between two targets will tend to be greater and less easily compensated for in a photographic system than in a scanner system.

7. The decrease with altitude of the signal-to-noise ratio will in general be greater for a photographic system than for a scanner system.

8. In general, the question of whether a camera or scanner system is better for a particular application can be answered only in light of the specific system's specifications, the conditions of data acquisition, the type of information desired, and the manner in which the system output must be processed or analyzed in order to obtain that information.

Appendix

Instrumentation and Calibration of the Airborne Multichannel Scanner

The multichannel scanning system operated in a C-47 aircraft at Willow Run Laboratories obtains simultaneous imagery in as many as 18 discrete channels in the spectral range from 0.32 to 13.5 μm. In addition, four P-2 aerial cameras provide photographic data using Plus-X pan film, infrared aerographic film, normal color film, and camouflage detection, false color film.

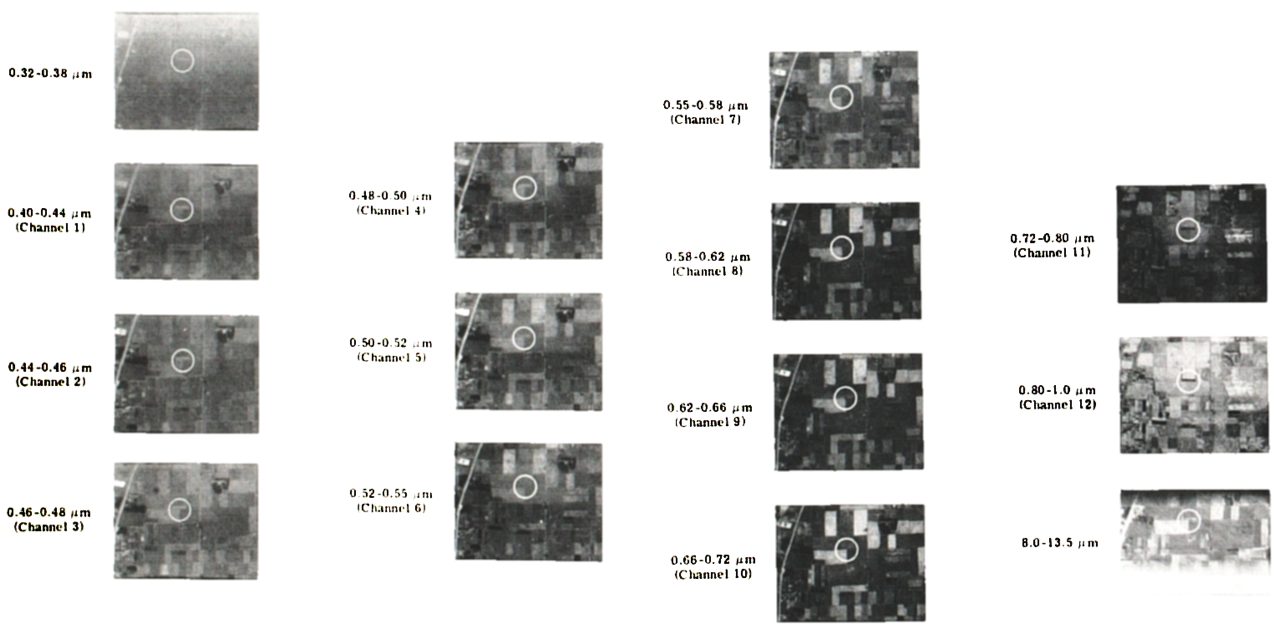

Fig. 9. Scanner imagery taken at an altitude of 8000 ft. Data acquired at 0850 hours on 15 September 1966.

The primary element of the system is a 12-channel spectrometer operating in the range from 0.4 to 1.0 μm. By employing a common aperture and prism dispersion to 12 photomultiplier detectors, truly instantaneous sensing of a given ground patch is achieved in 12 contiguous bands. In addition to the spectrometer, any three of the following detectors can be used at one time: a single-element detector operating at 0.32–0.38 μm; a three-element detector operating simultaneously at 1.0–1.4, 1.5–1.8, and 2.0–2.6 μm; a single-element detector operating 4.5–5.5 μm; and a single-element detector operating at 8.0–13.5 μm.

Calibration of the multispectral data is achieved using reference lamps and blackbody plates. The spectrometer and those detectors responsive to wavelengths of less than 2.6 μm are operated in one scanner housing which is equipped with two radiance-calibrated, quartz envelope, tungsten filament lamps. During each scan, the field of view looks sequentially at 80 angular degrees of ground data, the two calibration lamps, and the dark interior of the scanner housing. The thermal detectors sensitive to wavelengths greater than 4.5μm are normally operated in a second scanner housing. This housing is equipped with two temperature-controlled blackbody plates which are viewed sequentially with the ground scene, giving an apparent temperature calibration to the thermal imagery. Because of physical limitations on the positioning of these blackbody plates, the external angular field of view for imagery from this scanner is effectively limited to 35°.

For the present investigation, data recorded by the 12-channel spectrometer were analyzed in the laboratory using electronic sampling techniques. Electronic gating was used to retrieve samples of the signal for a given ground patch simultaneously from each of the 12 channels. An area-averaged signal for a given target was obtained by taking ten discrete samples from various points on the target. Clamping of the zero voltage level to the zero radiance level represented by the interior of the scanner housing resulted in 12 average signal voltages which were proportional to the average apparent radiance of the target in each channel. Similar sampling of the two calibration lamp signals provided two additional voltages for each channel which were proportional to the known radiances of the lamps. The variation of output voltage with radiance could then be determined and the target signals calibrated in terms of apparent radiance at the aperture of the system.

References

Higgins, G. C., and K. F. Stulte (1959), Experimental study of rms granularity as a function of scanning spot size, *J.O.S.A.* **49** (9), 925–929.

Holter, M. R., *et al.* (1962), *Fundamentals of Infrared Technology*, The MacMillan Company, New York, pp. 248–249.

Malila, W. A. (1968), Multispectral techniques for image enhancement and discrimination, *Photogrammetric Eng.* 34 (6), 566–575.

Middleton, W. E. K. (1958), *Vision through the Atmosphere*, University of Toronto Press, Toronto, Canada.

Received February 2, 1970
Revised version received May 11, 1970